Ion outflow observed by IMAGE: Implications for source regions and heating mechanisms

S. A. Fuselier[1], A. G. Ghielmetti[1], T. E. Moore[2], M. R. Collier[2], J. M. Quinn[3], G. R. Wilson[4], P. Wurz[5], S. B. Mende[6], H. U. Frey[6], C. Jamar[7], J.-C. Gerard[8], and J. L. Burch[9]

Abstract: Images of the Earth's proton aurora from the IMAGE spacecraft on 8 June 2000 indicate a temporally and spatially isolated ionospheric response to a shock that impinged on the Earth's magnetopause. Sometime after this ionospheric response, the Low Energy Neutral Atom imager on IMAGE detected enhanced ionospheric outflow. The time delay between the ionospheric response and the enhanced outflow is consistent with the travel time of ~30 eV neutral Oxygen (created by charge exchange of outflowing O^+ with the exosphere) from the low altitude ionosphere to the spacecraft. The prompt ionospheric outflow implies that the shock deposited sufficient energy in the topside ionosphere near or above the O^+ exobase to initiate the outflow.

Introduction

Since the identification of significant amounts of energetic O^+ in the magnetosphere [*Shelley et al.,* 1972], there has been much research on the acceleration mechanisms that permit this nominally gravitationally bound ion to exit the ionosphere. To date, statistical analysis of in situ observations have demonstrated that ion outflow is solar cycle [*Yau et al.,* 1985], seasonal [*Collin et al.,* 1998], and magnetospheric activity dependent [*Yau et al.,* 1985]. These and other studies of individual outflow events indicate that the ion acceleration mechanisms are altitude dependent and that there are probably several acceleration mechanisms ultimately responsible for ion outflow [e.g., *André and Yau*, 1997].

Energetic precipitating electrons deposit energy below the F peak (~120-200 km). While this creates ionization and heats the electron gas, the plasma is collision dominated [*Gombosi and Killeen*, 1987] so direct auroral energy input has minimal immediate effect on the topside F region plasma. After some time, this energy input can affect the topside F region, but time constants are >20 min.

In contrast, low energy electron precipitation deposits considerable energy into ionospheric electrons in the F region and topside up to the exobase (~350 - 1000 km, including charge exchange reactions). This effect enhances the ambipolar electric field, raises ionospheric scale heights, and accelerates light ion outflows [e.g., *Horwitz and Moore*, 1997]. In addition, fast auroral plasma winds driven by ion neutral coupling heat heavy ions strongly by ionospheric standards (~1-2 eV), increasing scale heights sufficient for heavy ions to escape gravity [*Heelis et al*., 1983]. This direct scale height increase from energy input at or near the exobase results in a rapid escape of ions from the ionosphere.

As 1-2 eV O^+ ions move to altitudes above 1000 km in the diverging magnetic field, they are affected by several mechanisms which heat them transversely (to the magnetic field) to energies ~10 eV. This transverse heating is believed to be dominated by broadband, low frequency turbulence with significant power near the heavy ion cyclotron frequency [*Klumpar et al.*, 1986; *André and Yau*, 1997]. Transverse acceleration is decisive in determining whether ions will escape Earth's gravity (which requires energies >10 eV) or will remain within an extended region of the ionosphere that is gravitationally and/or geomagnetically trapped. By far, the bulk of the escaping ionospheric O^+ is found in this transitional energy range [*Moore et al.*, 1986]. Thus, at altitudes of several thousand kilometers, there is an escaping O^+ population with a total flux of ~10^8-10^9 cm^{-2} s^{-1} [*Pollock et al.*, 1990] and a perpendicular temperature of ~10 eV [*Moore et al.*, 1986]. Fluxes at 50 (100) eV are more than 2 (5) orders of magnitude less than those at 10 eV.

At still higher altitudes, other wave-particle interactions and large-scale electric fields provide additional acceleration. However, the charge exchange probability rapidly decreases with altitude. For the purpose of this paper, this additional acceleration is not important because it simply speeds up the outflow without adding flux. Furthermore, it occurs well above the exobase and beyond the region where significant charge exchange creates low energy neutrals reported here.

Distinction between initial heating mechanisms that produce a delayed acceleration and those that produce a prompt acceleration require ion outflow measurements on timescales of a few minutes. This distinction is difficult using in situ measurements because the spacecraft moves across magnetic field lines where outflow can occur during a potential delay time of >20 min. This always produces the ambiguity that outflow may occur on field lines other than the ones that the in situ spacecraft is sampling. Thus, although it has been argued from in situ measurements that the ionospheric outflow is prompt [e.g., *Moore et al.*, 1999], this suggestion has not been conclusively verified.

The launch of the IMAGE mission, with its auroral imaging capabilities and new capability to image ionospheric ion outflow provides a unique opportunity to test initial ionospheric acceleration mechanisms. The purpose of this paper is to use these new imaging capabilities to investigate the timing between an impulsive input of energy into the ionosphere and the resulting ionospheric outflow.

Observations

IMAGE was launched on 25 March 2000 into a polar 7.2 R_E x 1000 km altitude elliptical orbit with initial apogee at ~12 LT and ~40˚ GSE latitude. The spacecraft carries a variety of neutral atom, radio plasma, and photon imagers [*Burch et al.*, 2000] including a Far Ultraviolet (FUV) Imager that makes the first global images of Doppler-shifted Lyman alpha emissions produced by energetic proton precipitation [*Mende et al.*, 2000]. Among the neutral atom imagers is a low energy neutral atom (LENA) imager which images ionospheric outflow in the energy range of 10 - 300 eV [*Moore et al.*, 2000].

The passage of a CME produced shock on 8 June 2000 provided an excellent opportunity to investigate outflow resulting from impulsive energy input into the ionosphere. At 0945 UT, the IMAGE spacecraft was at an altitude of ~6.6 R_E on the dawn flank of the magnetosphere. The location rotated into the $(Y^2+Z^2)^{1/2}$ - X_{GSM} plane along with the TY96 magnetic field is shown in Figure 1.

At 0905 UT, the CME produced shock passed the Wind spacecraft, located at +40 R_E X_{GSM} from the Earth. The solar wind velocity increased from 550 km/s to 700 km/s and the ion density increased from 2.5 cm^{-3} to 15 cm^{-3} across the shock front, resulting in an abrupt and substantial increase in the solar wind dynamic pressure. Given the X_{GSM} location of the Wind spacecraft and the solar wind speed, the disturbance propagating to and through the bow shock, across the magnetosheath to the magnetopause, and down the magnetic field line in the cusp would arrive at the ionosphere ~6-9 min after the shock front passed the Wind spacecraft.

Figure 2 shows two consecutive FUV images of the proton aurora (>1218Å Doppler-shifted Lyman-alpha emissions). The first image, at 0910:30 UT, shows weak auroral emissions with a slight enhancement near 12 LT. The second image (at 0912:30 UT) shows significant brightening at different latitudes but confined to the dayside region near 12 LT. This dramatic increase in the proton aurora coincides with the estimated arrival of the disturbance in the ionosphere that was produced by the interplanetary shock interaction with the magnetopause. The increase in emissions, likely produced by the precipitation of both magnetospheric and solar wind protons, provides a large, spatially distinct, and impulsive energy input into the ionosphere. Subsequent images (not shown) indicate decreased emissions near 12 LT but an overall brightening of the auroral oval.

Figure 3 shows the time history of the countrate from the Earth direction in the Oxygen time-of-flight channels of the LENA instrument. Prior to 0912 UT, the countrate in the Oxygen channels was consistent with background. A sharp increase in the countrate is seen at 0912:36 UT, coincident with the increase in the auroral emissions in Figure 2. A much larger increase in the countrate occurs 37.5 min after the brightening of the proton aurora.

Figure 4 shows two consecutive images of neutral Oxygen from the LENA imager from 0948 and 0950 UT, that is starting one spin (2 min) before the sharp increase in the Oxygen countrate in Figure 3. The dramatic increase in the Oxygen countrate in Figure 3 at 0950 UT comes from a region near, but slightly off the Earth direction.

The LENA imager uses conversion of low energy neutrals into negative ions at a conversion surface and subsequent electrostatic analysis of the negative ion [*Wurz et al.*, 1993]. With this detection technique, the instrument is susceptible to a variety of backgrounds [e.g., *Ghielmetti et al.*, 1994]. For example, there is an initial increase in the Oxygen countrate in Figure 3 coincident with the increase in the auroral emissions at 0912:30 UT in Figure 2. This countrate could be caused by an increase in the ultraviolet light from the bright aurora in Figure 2. Ultraviolet light can create negative ions through the release of photo-electrons and subsequent electron attachment to a neutral in the residual gas inside the

instrument. If this electron attachment occurs near the conversion surface and the negative ions have an energy of a few eV, then they will contribute to the instrument background. This background will be strongly correlated with photon flux. In addition, high energy (several keV) neutral H can sputter heavy negative ions with energies of a few eV off the conversion surface. These sputtered ions will be strongly correlated with the background energetic H flux. At 0912:36 UT, the neutral H countrate also increases dramatically. Thus, the initial signal at 0912:36 UT in Figure 3 may not be Oxygen outflow from the ionosphere due to the impulsive energy input into the ionosphere seen in Figure 2.

In contrast, the dramatic increase in the Oxygen countrate at 0950 UT in Figure 3 has no corresponding increase in auroral photon intensity for the entire period between 0912:30 and 0950 UT (not shown). This increase also does not have an associated rapid increase in the neutral Hydrogen countrate of comparable magnitude (also not shown).

The LENA instrument was designed with relatively crude energy resolution within the energy passband. Unfortunately, problems with the energy discrimination in the LENA instrument resulted in the inability to measure Oxygen energies for this time period. Fortunately, the ion optics and the voltage settings of the instrument limit the incident neutral energy to a relatively narrow window between 10 eV and ~150 eV in the normal detection process (i.e., conversion of incident low energy neutral Oxygen into negative ions and subsequent analysis of these ions by the instrument). However, as discussed above, energetic neutrals could sputter negative ions from the conversion surface. This and other possible backgrounds will be considered in the discussion section.

Here, it is assumed that the sharp increase in the countrate at 0950 UT was caused by an increase in 10 to 150 eV neutral Oxygen flux. Neutrals with these energies are created by charge exchange of the ionospheric O^+ outflow with the Earth's exosphere. With this assumption, the travel times from the ionosphere to the spacecraft (a distance of 6.6 R_E, see Figure 1) for different energy neutrals is shown in Table 1.

Within the nominal passband of the instrument, Oxygen travel times vary from 15 min to 1 hour. Since the H energy passband of the instrument is the same, H travel times are simply a factor of 4 smaller in Table 1. The 37.5 min delay between the ionospheric disturbance and the large Oxygen signal increase in Figure 3 is consistent with the travel time of 30 eV Oxygen neutrals from the ionosphere to the spacecraft. For this energy neutral, there is no delay between the ionospheric disturbance and the initiation of ionospheric outflow.

Discussion

Figure 2 shows that there was a localized response in the ionosphere due to the compression of the magnetosphere by a CME shock front. The ionosphere is disturbed over a considerable range of latitude but a relatively small range of local time near 12 LT. Neutral atom observations from the IMAGE spacecraft, located 6.6 R_E from this ionospheric disturbance, show a dramatic increase in the Oxygen channel countrate from the general direction of the Earth (Figure 4).

This increase occurs 37.5 min after the ionospheric disturbance, consistent with the travel time of 30 eV neutral Oxygen from the ionosphere to the spacecraft (Table 1). If the increased countrate is due to these energy neutrals, then there is no time delay between the ionospheric disturbance and the initiation of ion outflow from the ionosphere.

Because the LENA imager does not have energy resolution in its 10 to 150 eV energy passband, it is possible that the 37.5 min time delay could be accounted for by a delay in the initiation of the ion outflow and the travel time of higher energy neutral Oxygen or Hydrogen (see Table 1). Energetic Hydrogen can produce measurable counts in the Oxygen channels of the instrument by sputtering of negative heavy ions off the conversion surface. As discussed above, heavy ion sputtering by Hydrogen could have caused the increase in the Oxygen channel countrate at 0912:30 UT in Figure 3, coincident with the arrival time of the ionospheric disturbance.

While there is no direct evidence from the IMAGE observations in Figures 2 through 4 to discount the possibility that higher energy neutrals cause the increased countrate at 0950 UT, results from previous modeling and in situ observations of ion outflow suggest that this is not the case. Modeling of the ionospheric response to an impulsive heating event indicates that there is a significant response from ionospheric O^+ but essentially no response by ionospheric H^+ [*Gombosi and Kileen,* 1987]. Furthermore, there was no corresponding increase in the H countrate at 0950 UT, coincident with the Oxygen countrate increase. Thus, it is likely that the increase in the countrate at 0950 UT is due to direct detection of ionospheric Oxygen and not H sputtering of Oxygen off the conversion surface.

Neutral Oxygen is produced by charge exchange of the outflowing O^+ distribution with the Earth's exosphere. In situ observations indicate that the outflowing O^+ distribution from the ionosphere has a relatively low temperature (~10 eV) and fluxes at 50 (100) eV are more than 2 (5) orders of magnitude less than that those 10 eV [*Moore et al.,* 1986, Figure 9]. These observations suggest that the neutral Oxygen observed by LENA at 0950 UT had an energy less than 50 eV. Typical fluxes of escaping ionospheric O^+ are ~10^8-10^9 $cm^{-2}s^{-1}$ [*Pollock et al.,* 1990]. While considerable modeling will be required to determine the resulting neutral flux, the observed peak countrate in Figure 3 is roughly consistent with typical fluxes of escaping ionospheric O^+ [see, *Moore et al.,* 2000].

As discussed in the introduction, enhanced precipitation that deposits energy below the F peak (~120-200 km) will affect the topside ionosphere up to the exobase (~350 - 1000 km) only after a time delay exceeding 20 min. The interpretation of the data in this paper leads to the conclusion that the ionospheric outflow was prompt in response to the enhanced energy input. This does not rule out the possibility that sustained ion outflow results from energy input at lower altitudes. However, direct topside ionospheric heating or some similar mechanism appears to be providing the magnetosphere with significant and nearly instantaneous ionospheric outflow in response to the passage of a CME shock.

Acknowledgments: The authors thank W. K. Peterson for his helpful comments. Solar wind data was obtained from the CDAWeb from K. Ogilvie. Research on the IMAGE mission is supported by NASA contract to Southwest Research Institute and subcontracts to participating IMAGE institutions.

References

André, M., and Yau, A. L., Theories and observations of ion energization and outflow in the high latitude magnetosphere, *Space Sci. Rev., 80*, 27, 1997.

Burch, J. L., IMAGE mission overview, *Space Sci. Rev., 91*, 1, 2000.

Collin, H. L., W. K. Peterson, O. W. Lennartsson, J. F. Drake, The seasonal variation of auroral ion beams, *Geophys. Res. Lett., 25*, 4071, 1998.

Ghielmetti, A. G., E. G. Shelley, S. A. Fuselier, P. Wurz, P. Bochsler, F. A. Herrero, M. F. Smith, and T. S. Stephen, Mass spectrograph for imaging low-energy neutral atoms, *Optical Eng., 33*, 362, 1994.

Gombosi, T. I., and T. L. Kileen, Effects of thermospheric motions of the polar wind: A time-dependent numerical study, *J. Geophys. Res., 92*, 4725, 1987.

Heelis, R. A., G. J. Bailey, R. Sellek, R. J. Moffett, and B. Jenkins, Field-aligned drifts in subauroral ion drift events, *J. Geophys. Res., 98*, 21493, 1993.

Horwitz, J. L., and T. E. Moore, Four contemporary issues concerning ionospheric plasma flow to the magnetosphere, *Space Sci. Rev., 80*, 49, 1997.

Klumpar, D. M., A digest and comprehensive bibliography on transverse auroral ion acceleration, in *Ion Acceleration in the Magnetosphere and Ionosphere*, Geophys. Monogr., American Geophysical Union, 389, 1986.

Mende, S. B., et al., Far ultraviolet imaging from the IMAGE spacecraft: 3. Spectral imaging of Lyman-alpha and OI 135.6 nm, *Space Sci. Rev., 287*, 2000.

Moore, T. E., M. Lockwood, M. O. Chandler, J. H. Waite Jr., C. R. Chappell, A. Persoon, and M. Sugiura, Upwelling O^+ ion source characteristics, *J. Geophys. Res., 91*, 7019, 1986.

Moore, T. E., et al., Ionospheric mass ejection in response to a CME, *Geophys. Res. Lett., 26*, 2339, 1999.

Moore, T. E., et al., The low energy neutral atom imager for IMAGE, *Space Sci. Rev., 155*, 2000.

Pollock, C. J., M. O. Chandler, T. E. Moore, J. H. Waite, Jr., C. R. Chappell, and D. A. Gurnett, A survey of upwelling ion event characteristics, *J. Geophys. Res., 95*, 18,969, 1990.

Shelley, E. G., Johnson, R. D., and R. D. Sharp, Satellite observations of energetic heavy ions during a geomagnetic storm, *J. Geophys. Res., 77*, 6104, 1972.

Wurz, P., et al., Concept of the HI-LITE Neutral Atom Imaging Instrument, Proceedings of the Symposium on Surface Science, eds. P. Varga, and G. Betz, pp. 225-230, Kaprun, Austria, 1993.

Yau, A. W., Shelley, E. G., Peterson, W. K., and L. Lenchyshyn, Energetic auroral and polar ion outflow at DE-1 altitudes: Magnitude, composition, magnetic activity dependence and long-term variations, *J. Geophys. Res., 90*, 8417, 1985.

S. A. Fuselier, and A. G. Ghielmetti, Lockheed Martin Advanced Technology Center, Dept. L9-42 Bldg. 255, 3251 Hanover St., Palo Alto, CA 94304. (e-mail: fuselier@spasci.com, gmetti@cobra.spasci.com)

T. E. Moore, and M. R. Collier, Goddard Space Flight Center, Code 692, Greenbelt, MD 20771. (e-mail: thomas.e.moore@gsfc.nasa.gov)

J. M. Quinn, Morse Hall University of New Hampshire, Durham, NH 03824 (e-mail: jack.quinn@unh.edu).

G. R. Wilson, Mission Research Corporation, 1 Tara Blvd Ste 302, Nashau, NH 03062 (e-mail: gwilson@mrcnh.com).

P. Wurz, University of Bern, Physikalisches Institut, Sidlerstrasse 5, CH-3012 Bern, Switzerland. (e-mail: peter.wurz@soho.unibe.ch)

S. B. Mende, and H. U. Frey, Space Science Lab, University of California, Berkeley, CA 94720. (e-mail: mende@apollo.ssl.berkeley.edu)
C. Jamar, Centre Spatiale de Liège, Liège, B 4000 Belgium. (e-mail: cjamar@ulg.ac.be)
J.-C. Gerard, 5 Ave Cointe, University of Liège, Liège, B 4000 Belgium. (e-mail: gerard@astro.ulg.ac.be)
J. L. Burch, Southwest Research Institute, 6220 Culebra Rd., San Antonio, TX. (e-mail: jburch@swri.edu)

(Received October 5, 2000; revised December 13, 2000; accepted January 12, 2001.)

[1] Lockheed Martin Advanced Technology Center, Palo Alto, CA

[2] Goddard Space Flight Center, Greenbelt, MD

[3] University of New Hampshire, Durham, NH

[4] Mission Research Corporation, Nashau, NH

[5] University of Bern, Bern, Switzerland

[6] University of California, Berkeley, CA

[7] Centre Spatiale de Liège, Liège, Belgium

[8] University of Liège, Liège, Belgium

[9] Southwest Research Institute, San Antonio, TX

FUSELIER ET AL.: IMPLICATIONS OF ION OUTFLOW

FUSELIER ET AL.: IMPLICATIONS OF ION OUTFLOW

FUSELIER ET AL.: IMPLICATIONS OF ION OUTFLOW

FUSELIER ET AL.: IMPLICATIONS OF ION OUTFLOW

FUSELIER ET AL.: IMPLICATIONS OF ION OUTFLOW

Figure 1. The location of the IMAGE spacecraft in the magnetosphere at the time of a passage of a CME-related shock. The spacecraft was located at approximately 9 LT, 6.6 R_E from the Earth. The projection of the magnetic field line from the TY96 model is shown.

Figure 2. Two consecutive snapshots of the proton aurora (Doppler shifted Lyman-alpha emissions). The ionospheric response to the CME shock passage is evident in the second image. There is a significant and localized brightening of the emissions near 12 LT.

Figure 3. Countrate in the Oxygen channels of the LENA imager from the direction of the Earth. A prompt countrate increase occurs at the time of the enhanced proton aurora in

Figure 2. A much larger increase in the countrate is seen 37.5 min after the initial ionospheric disturbance.

Figure 4. Two consecutive images from the LENA imager from the Earth direction. These images show how the dramatic increase in the Oxygen countrate (Figure 3) comes from slightly off the direction of the Earth.

Figure 1. The location of the IMAGE spacecraft in the magnetosphere at the time of a passage of a CME-related shock. The spacecraft was located at approximately 9 LT, 6.6 R_E from the Earth. The projection of the magnetic field line from the TY96 model is shown.

Figure 2. Two consecutive snapshots of the proton aurora (Doppler shifted Lyman-alpha emissions). The ionospheric response to the CME shock passage is evident in the second image. There is a significant and localized brightening of the emissions near 12 LT.

Figure 3. Countrate in the Oxygen channels of the LENA imager from the direction of the Earth. A prompt countrate increase occurs at the time of the enhanced proton aurora in Figure 2. A much larger increase in the countrate is seen 37.5 min after the initial ionospheric disturbance.

Figure 4. Two consecutive images from the LENA imager from the Earth direction. These images show how the dramatic increase in the Oxygen countrate (Figure 3) comes from slightly off the direction of the Earth.

Table 1: Travel Times for Neutrals from the Ionosphere

Energy (eV)	O Travel Time (min)	H Travel Time (min)
10	64.4	16.2
30	37.1	9.3
50	28.5	7.2
100	20.3	5.1
150	16.6	4.1

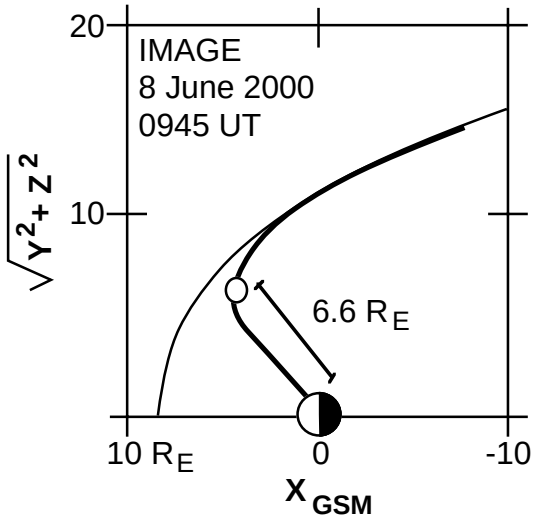

Figure 1

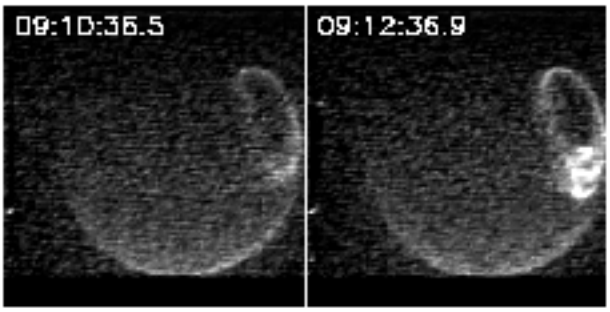

Figure 2

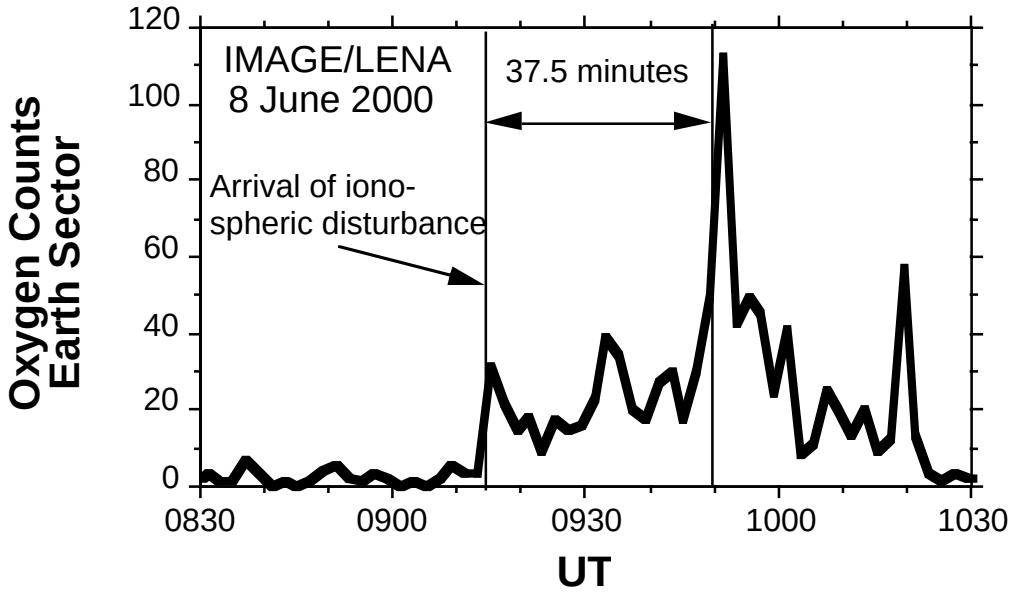
IMAGE/LENA
8 June 2000
37.5 minutes
Arrival of iono-
spheric disturbance
Oxygen Counts
Earth Sector
120
100
80
60
40
20
0
0830
0900
0930
1000
1030
UT

Figure 3

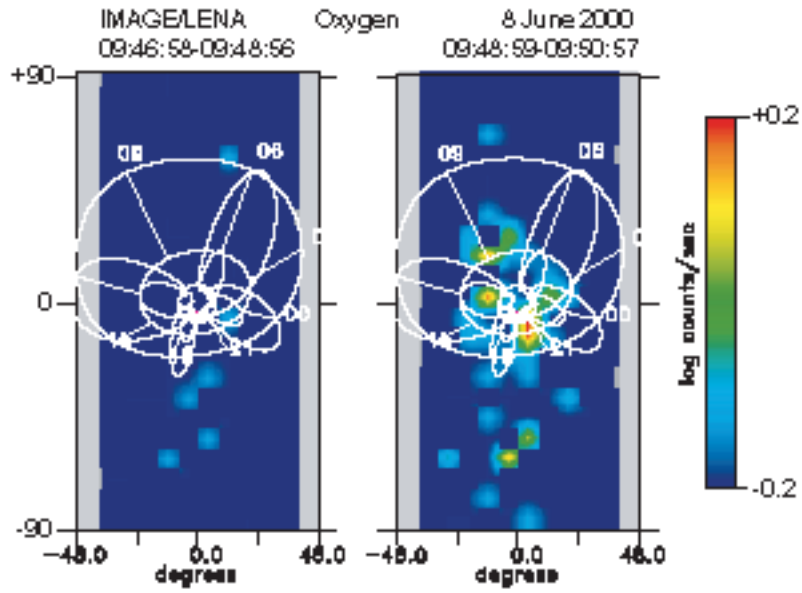
IMAGE/LENA
Oxygen
8 June 2000
09:46:58-09:48:56
09:48:59-09:50:57
+90
0
-90
08
08
08
08
-48.0
0.0
48.0
degrees
-48.0
0.0
48.0
degrees
+0.2
-0.2
log counts/sec

Figure 4